

¹ Cellects: a software to quantify cell expansion and motion

³ **Aurèle Boussard**  ^{1,2,3}¶, **Manuel Petit**  ², **Patrick Arrufat**  ¹, **Audrey Dussutour**  ¹, and **Alfonso Pérez-Escudero**  ¹

⁵ **1** Research Centre on Animal Cognition (CRCA), Centre for Integrative Biology (CBI), Toulouse University, CNRS  ⁶ Morphogenesis Simulation and Analysis In silico (MOSAIC), Plant development and reproduction (RDP), École normale supérieure (ENS) de Lyon  ⁷ **3** Jacques Louis Lions Laboratory (LJLL), Sorbonne Université, Paris  ⁸ Corresponding author

DOI: [10.xxxxxx/draft](https://doi.org/10.xxxxxx/draft)

Software

- [Review](#) 
- [Repository](#) 
- [Archive](#) 

Editor: 

Submitted: 13 February 2026

Published: unpublished

License

Authors of papers retain copyright and release the work under a Creative Commons Attribution 4.0 International License ([CC BY 4.0](https://creativecommons.org/licenses/by/4.0/))

⁹ Summary

¹⁰ Cellects is a user-friendly and open-source software for automated quantification of biological growth, motion, and morphology from 2D image data and time-lapse sequences (2D + t), acquired under a wide range of experimental conditions and biological systems (from ¹¹ fungal colonies to unicellular branching networks). The software is available as a stand-alone ¹² version, featuring a graphical interface that supports interactive parameter tuning, visualization, validation, and batch processing. The analysis pipeline can be extended and customized using ¹³ a dedicated Python API.

¹⁷ The typical inputs and outputs are as follows. Cellects is designed to process grayscale or color ¹⁸ images originating from standard microscopy, macroscopic imaging setups, or camera-based ¹⁹ platforms. The software supports single or multiple organisms growing or moving in one or ²⁰ several arenas and can analyze multiple folders sequentially. All quantitative results (area, ²¹ circularity, orientation axes, centroid trajectories, oscillations, network topology...) are exported ²² as standardized .csv files suitable for downstream statistical analysis, ensuring reproducibility ²³ and integration into existing workflows.

²⁴ Statement of need

²⁵ Modern imaging generates high-resolution biological datasets across scales, yet automated ²⁶ analysis remains challenging for non-experts, necessitating accessible tools.

²⁷ Cellects is suited to biological systems exhibiting continuous growth, deformation, or collective ²⁸ motion, such as fungal colonies (Figure 1a-d), HeLa cells (Figure 1e-h), and slime molds ²⁹ (Figure 1i-n). By contrast, most existing tools target single species (mainly yeast or bacteria) ³⁰ and fail to generalize to heterogeneous morphologies such as branching slime mold networks or ³¹ collective cellular movement during proliferation.

³² Open source alternatives often lack graphical user interfaces (GUIs) and robust automation ³³ under variable lighting/contrast conditions, while commercial platforms often require ³⁴ preprocessing or post-analysis using additional software, compromising reproducibility.

³⁵ By combining dynamic segmentation algorithms with a modular pipeline (see Software Design), ³⁶ Cellects supports both single-specimen analysis and high-throughput multi-arena experiments, ³⁷ outputting standardized metrics directly usable in downstream statistical workflows. While ³⁸ enabling reproducible studies across diverse biological models, this automated quantification ³⁹ reduces observer bias.

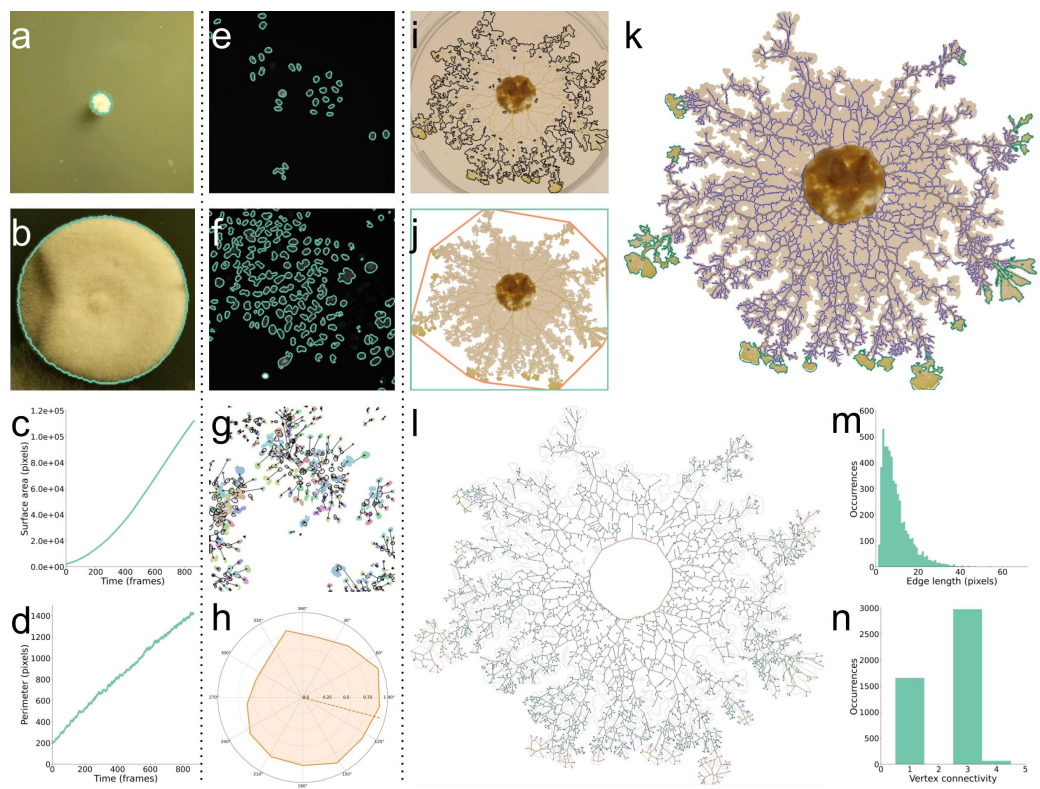


Figure 1: Cellular dynamics and morphologies across systems. **a,b)** Fungal growth (unknown sp.) from initial (a) to final (b) stages with green segmentation contours, from (Peñil Cobo et al., 2018); **c,d)** Corresponding area and perimeter curves over time (c: area, d: perimeter). **e,f)** Tracking of HeLa “Kyoto” cells marked with mCherry-H2B, from (Guillet, 2022) showing initial (e) and final (f) images with segmentation contours. **g)** Motion vectors (arrows) of the 250 most mobile cells among 1319 detected (black contour: original positions, colored-filled patches: final locations). **h)** Spider plot representing HeLa cell movement directions. **i,j)** *Physarum polycephalum* morphology after 16:40 hours of exploration (this study). (h: cell segmentation, i: convex hull (orange) and bounding rectangle (green)). **k,l)** Network segmentation (j: blue network; turquoise pseudopods) and graph reconstruction (k: edges colored by width from blue to red, green branching vertices, black tips, yellow food vertices). **m,n)** *Physarum* connectivity metrics: edge lengths (l) and vertex degrees (m). Panels a-d (fungus), e-h (HeLa), i-n (*Physarum*).

40 State of the field

41 Collects fills three major gaps in existing tools:

Limitation	Existing solution	Collects innovation
Taxon-specific design	Bacteria (Ernebjerg & Kishony, 2012), Yeast (Falconnet et al., 2011)	Universal pipeline adaptable to fungi, animals, and slime molds via tunable segmentation parameters
Interface barriers	Manual scripting (Pandey et al., 2021), Commercial solutions (ScanLag (Levin-Reisman et al., 2014) or ColTapp (Bär et al., 2021))	GUI + API dual architecture for both non-programmers and developers
Output limitations	Needs post-analysis manual processing with tools like ImageJ/Fiji (Schneider et al., 2012)	Precomputed shape descriptors, network topology data (vertex degrees, edge widths), and CSV exports

42 While commercial tools prioritize ease of use over customization, open-source platforms often
43 require manual scripting. Cellects bridges this divide by combining automation with a validation
44 tool for result refinement, enabling robust and accessible analysis of growth dynamics across
45 biological systems and fostering reproducibility and cross-disciplinary research.

46 Software design

47 The software is organized around a layered architecture centered on a global controller
48 (*ProgramOrganizer*), which maintains experiment state, configuration parameters, and
49 processing context. This controller can be driven either through the graphical user interface or
50 programmatically.

51 The graphical interface follows a sequential workflow implemented via a stacked widget
52 (*CellectsMainWidget*), exposing successive stages for data loading (*FirstWindow*),
53 segmentation and arena definition (*ImageAnalysisWindow*), and time-series execution
54 (*VideoAnalysisWindow*). This structure mirrors the experimental pipeline and limits user
55 interaction to valid analysis states while allowing iterative refinement at each step. To balance
56 accessibility with flexibility, novice users benefit from an automated parameter search during
57 initial setup (in *ImageAnalysisWindow*), while experienced ones can bypass default algorithms
58 in advanced mode to directly customize image processing settings.

59 Static and temporal analyses are separated through two dedicated classes: *OneImageAnalysis*,
60 responsible for preprocessing tasks such as greyscale conversion, filtering and background
61 subtraction, and *MotionAnalysis*, which performs segmentation, post-processing, video-based
62 measurements and temporal feature extraction. This separation allows computationally intensive
63 motion analysis to build upon validated segmentation results.

64 Cellects targets diverse biological datasets (e.g., Fungi, HeLa cells, Myxamoebae) acquired under
65 variable imaging conditions. Rather than relying on a single segmentation model, the image
66 analysis layer provides automated and configurable pipelines combining multiple color-space
67 representations, image filtering, K-means clustering and threshold-based methods. Geometric
68 descriptors (area, perimeter, circularity) are encapsulated in the *ShapeDescriptors* class, while
69 additional modules support graph-based dynamics, oscillatory behavior, and morphological
70 operations.

71 To maintain interactivity during heavy computation, Cellects combines Qt-based threading
72 for GUI responsiveness with multiprocessing for video analysis. Memory usage is explicitly
73 managed through sequential image processing and controlled data release.

74 Research impact statement

75 Related work

76 Cellects' lineage traces directly to [Vogel2015]'s MATLAB implementation, with an early
77 iteration already employed by [Boussard2019]. While the final version has not yet enabled new
78 studies, it has been developed to address specific research questions from (Boussard et al.,
79 2021) and from an ongoing ANR project (ANR-24-CE45-3362, PI Claire David).

80 Validation

81 The software's robustness is demonstrated through specimen and background accuracies (Figure
82 2) in diverse contexts. First, manual segmentation of Figure 1 examples provided ground truth
83 for canonical cases: single fungus on color-varying background Figure 2a-c, multi-specimen
84 tracking Figure 2d-f with microscopy data, and network extraction Figure 2g-i. Second, Cellects
85 was tested on highly heterogeneous cells where manual distinction is infeasible. Accuracy was
86 estimated via error annotations (Figure 2j) comparing original images to results, achieving

⁸⁷ >97% accuracy across five challenging conditions ([Figure 2k](#): high contrast + optimal setup,
⁸⁸ heterogeneous colors, low contrast + desiccation, low contrast + optimal, very low resolution)
⁸⁹ through iterative parameter refinement in the GUI.

⁹⁰ Applications span fungal growth tracking ([Figure 1a-d](#), ([Peñil Cobo et al., 2018](#))), HeLa cells
⁹¹ motion ([Figure 1e-h](#), ([Guillet, 2022](#))), and network analysis of *P. polycephalum* ([Figure 1i-n](#),
⁹² this study), highlighting adaptability to diverse biological systems and imaging setups.

DRAFT

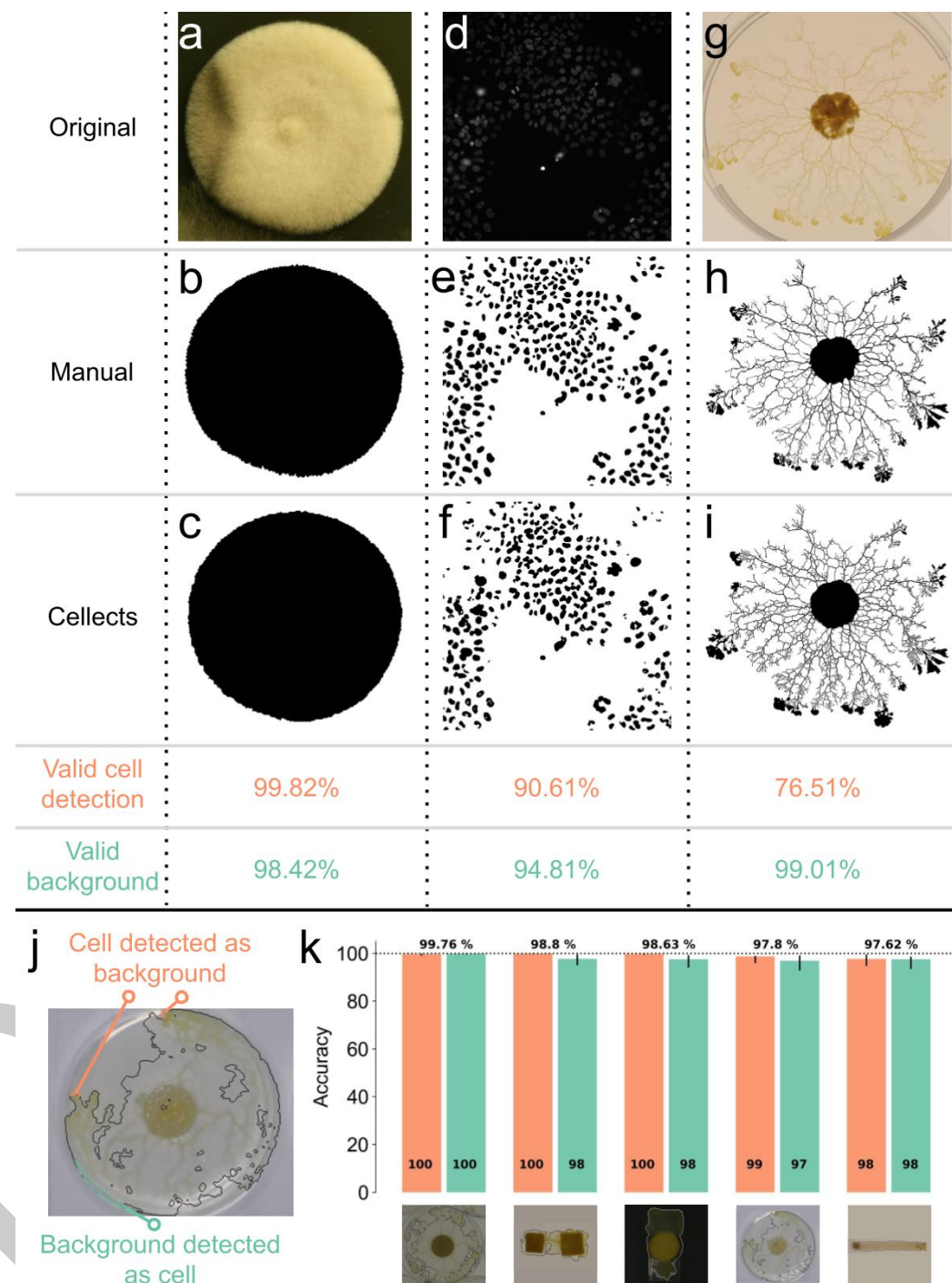


Figure 2: Validation of Cellects across five experimental conditions. **a,b,c)** Segmentation accuracy of the fungi (Peñil Cobo et al., 2018) against ground truth: original image (a) was used to create a mask manually (b) and using Cellects (c). The valid cell detection is the percentage of pixels accurately labelled as cells by Cellects. The valid background is the percentage of pixels accurately labelled as background by Cellects. **d,e,f)** Segmentation accuracy of the Hela "Kyoto" cells (Guillet, 2022) against ground truth. **g,h,i)** Segmentation accuracy of the *P. polycephalum* network against ground truth (this study). **j)** Image of a *P. polycephalum* plasmodia, showing the two types of errors detected during validation: background pixels classified as cell (orange), cell pixels classified as background (green). **k)** A posteriori accuracy in 5 experimental conditions (shown below the bars): high contrast with optimal setup, high contrast with heterogeneous colors, low contrast with a setup prone to desiccation, low contrast with optimal setup, low resolution. Orange: Proportion of cell pixels correctly identified as cell. Green: Proportion of background pixels correctly identified as background. Error bars show the 95% confidence interval. Percentages on top show the average of both bars.

⁹³ Acknowledgements

⁹⁴ We thank Audrey Bizet for her work on the first experiment of [Figure 2e](#), Charlotte Dupont
⁹⁵ and Paul-Antoine Badon for the second experiment of [Figure 2e](#), Nirosha Murugan for her
⁹⁶ help with the fourth experiment of [Figure 2e](#), Ana Lucía Morán Hernández for her help with
⁹⁷ the fifth experiment of [Figure 2e](#), and Florent Le Moël, Rémi Giorno dit Journo, Guillaume
⁹⁸ Cerutti, Jonathan Legrand, and Olivier Ali for their help during software development.

⁹⁹ Funding

¹⁰⁰ A.B. was supported by grants from the ‘Agence Nationale de la Recherche’ (ANR-17-CE02-
¹⁰¹ 0019-01-SMARTCELL, PI A.D. and ANR-24-CE45-3362, PI Claire David). A.D. acknowledges
¹⁰² support by the CNRS. APE acknowledges support from a CNRS Momentum grant and an
¹⁰³ ANR JCJC grant (ANR-22-CE02-0002, ForAnInstant).

¹⁰⁴ The funders had no role in study design, data collection and analysis, the decision to submit
¹⁰⁵ the work for publication, or preparation of the manuscript.

¹⁰⁶ Author contribution

¹⁰⁷ Conceptualization, A.B., P.A., A.D., A.P.E.; methodology, A.B., M.P., A.P.E, P.A.; software,
¹⁰⁸ A.B.; investigation, A.B., A.D.; resources, A.B., P.A., A.D., A.P.E.; writing – original draft
¹⁰⁹ preparation, A.B.; writing – review and editing, A.B., A.P.E., M.P., A.D.; visualization, A.B.;
¹¹⁰ supervision, P.A., A.D., A.P.E.; project administration, A.B.; funding acquisition, A.D., A.P.E.

¹¹¹ AI usage disclosure

¹¹² The generative model ‘Devstral-Small-2507’ was used to generate initial drafts of function
¹¹³ docstrings and propose unit test templates. All AI-generated content underwent manual
¹¹⁴ verification to ensure alignment with function usages in the context of real datasets.

¹¹⁵ Data availability

¹¹⁶ Lead contact

¹¹⁷ Aurèle Boussard: aurele.boussard@gmail.com, ORCID: 0000-0002-6083-4272

¹¹⁸ Data and code availability

¹¹⁹ The Windows and macOS versions are accessible via the following link: <https://github.com/Aurele-B/Cellects/releases>.

¹²¹ The software documentation is available at <https://aurele-b.github.io/Cellects> and its source
¹²² code can be found at <https://github.com/Aurele-B/Cellects>.

¹²³ To access the data and replication code, refer to: <https://datadryad.org/stash/share/nCvWIZoZ8-Wnxm0CjnPbbznUPw90RYdo1YVJEQkfLIY>

¹²⁵ References

¹²⁶ Bär, J., Boumasmoud, M., Kouyos, R. D., Zinkernagel, A. S., & Vulin, C. (2021). Author
¹²⁷ correction: Efficient microbial colony growth dynamics quantification with ColTapp, an

- 128 automated image analysis application. *Scientific Reports*, 11, 6050. <https://doi.org/10.1038/s41598-021-85033-8>
- 129
- 130 Boussard, A., Fessel, A., Oettmeier, C., Briard, L., Döbereiner, H.-G., & Dussutour, A. (2021).
131 Adaptive behaviour and learning in slime moulds: The role of oscillations. *Philosophical
132 Transactions of the Royal Society B*, 376(1820), 20190757. [https://doi.org/10.1098/rstb.2019.0757](https://doi.org/10.1098/rstb.
133 2019.0757)
- 134 Ernebjerg, M., & Kishony, R. (2012). Distinct growth strategies of soil bacteria as revealed by
135 large-scale colony tracking. *Applied and Environmental Microbiology*, 78(5), 1345–1352.
136 <https://doi.org/10.1128/AEM.06585-11>
- 137 Falconnat, D., Niemistö, A., Taylor, R., Ricicova, M., Galitski, T., Shmulevich, I., & Hansen, C.
138 L. (2011). High-throughput tracking of single yeast cells in a microfluidic imaging matrix.
139 *Lab on a Chip*, 11(3), 466–473. <https://doi.org/10.1039/COLC00228C>
- 140 Guiet, R. (2022). *HeLa "kyoto" cells under the scope* (Version v0) [Data set]. Zenodo.
141 <https://doi.org/10.5281/zenodo.6139958>
- 142 Levin-Reisman, I., Fridman, O., & Balaban, N. Q. (2014). ScanLag: High-throughput
143 quantification of colony growth and lag time. *Journal of Visualized Experiments: JoVE*,
144 89, 51456. <https://doi.org/10.3791/51456>
- 145 Pandey, S., Park, Y., Ankita, A., & Phillips, G. J. (2021). Scan4CFU: Low-cost, open-source
146 bacterial colony tracking over large areas and extended incubation times. *HardwareX*, 10,
147 e00249. <https://doi.org/10.1016/j.johx.2021.e00249>
- 148 Peñil Cobo, M., Libro, S., Marechal, N., D'Entremont, D., Peñil Cobo, D., & Berkmen,
149 M. (2018). Visualizing bacterial colony morphologies using time-lapse imaging chamber
150 MOCHA. *Journal of Bacteriology*, 200(2), 10–1128. <https://doi.org/10.1128/jb.00413-17>
- 151 Schneider, C. A., Rasband, W. S., & Eliceiri, K. W. (2012). NIH image to ImageJ: 25 years of
152 image analysis. *Nature Methods*, 9(7), 671–675. <https://doi.org/10.1038/nmeth.2089>